http://dx.doi.org/10.5012/bkcs.2012.33.2.449

Charge Transport Properties of Polyaniline-gold/graphite Oxide Composite Films

C. Basavaraja, Won Jung Kim, P. X. Thinh, and Do Sung Huh*

Department of Chemistry and Institute of Basic Science, Inje University, Kimhae, Kyungnam 621-749, Korea
**E-mail: chemhds@inje.ac.kr*
Received September 23, 2011, Accepted November 29, 2011

A polyaniline-gold composite was prepared *via* the polymerization of aniline hydrochloride with or without water-soluble graphite oxide using auric acid as an oxidant. The reaction products were characterized using X-ray photoelectron spectroscopy. The thermal stability and embedded crystallinity of the composites were also investigated using thermogravimetric and X-ray diffraction analyses. The electrical properties of the composites were examined using cyclic voltammetric measurements at room temperature and temperature-dependent DC conductivity within 300-500 K. Compared to pure graphene oxide and polyaniline-gold composite, the polyaniline-gold-graphene composite exhibited higher crystallinity and thermal stability, and higher current density response under equivalent conditions.

Key Words : Electrical properties, Polyaniline, Graphene oxide, Gold nanoparticles (GNPs)

Introduction

Conductive polymers such as polyaniline (PANI),[1] polypyrrole,[2] polythiophene, and their derivatives[3] have been extensively studied as potential supercapacitors. Among these polymers, PANI is considered the most promising material because of its high capacitive characteristic, low cost, and ease of synthesis.[4,5] Previous studies demonstrated that PANI composites with metal oxides showed improved supercapacitor performance.[6] Among the metal nanoparticles, gold has been widely used because of its unique optical and catalytic properties.[7] Thus, PANI-gold composite exhibits a combination of the desirable qualities of both components, namely, good stability, high conductivity, and the unique optical properties of the metal component, in addition to easy processing, light weight, variable conductivity through doping, and the excellent optical properties of the polymer. However, many of these composites have a small surface area. The metal nanoparticles are dispersed throughout the entire PANI matrix. Intimate contact between the metal nanoparticles and PANI matrix is weak and very difficult to establish a strong interaction between PANI and metal nanoparticles. This may be because PANI and metal nanoparticles are heterogeneous materials wherein the intermixing of these two materials results in a very weak interaction between them. Contact between metal particles and the polymer is crucial in molecular electronic devices because the charge transfer at the contact point plays an important role in its functionality.

Incorporation of metal nanoparticles into the polymer matrix is a field of particular interest for materials engineering and for the study of nanoparticle-matrix interactions.[8] Although there are many complexes of ligand-stabilized metal nanoparticles, there are few examples of polymer stabilized metal nanoparticles in which the metal nanoparticles are functionalized by the polymer.[9] There have been a variety of attempts to make nanoparticle-polymer composites. Overall, we note four different approaches used to date. The first technique comprises the preparation of metal nanoparticles in the polymer matrix by the reduction of metal salts in the polymer matrix.[10] The second technique consists of polymerizing the organic monomer around the preformed metal nanoparticles.[11] The third approach has involved the blending of preformed nanoparticles into a pre-synthesized polymer.[12] The fourth procedure is the most desirable approach in order to achieve an intimate contact between the metal and the polymer, and it involves the blending of a monomer and a metal salt.[13] The choice of the metal salt and the monomer should be such that the metal salt can oxidize the monomer to form a polymer as well as utilize the electrons released during the oxidation to reduce the metal salt to form metal nanoparticles.

Graphene is a two-dimensional form of graphite that has attracted considerable interest [14-17] because of its high surface area, excellent mechanical properties, and conductivity.[18,19] Graphene oxide is a single sheet of graphite oxide bearing oxygen functional groups on the basal planes and at the edges. It can be obtained *via* exfoliation of graphite oxide (GO).[20] In general, incorporation of GO in the polymer matrix can lead to improvements in the mechanical and thermal properties of materials, especially in the enhancement of electrical conductivity. Therefore, we have earlier reported on the simple synthesis and characterization of PANI-GNP-GO composite.[21]

In this paper, the synthesized PANI-GNP-GO nanocomposites were studied by thermogravimetric analysis (TGA) for thermal stability, and further studied by X-ray diffraction (XRD) and X-ray photoelectron spectroscopy (XPS) analysis for the crystallinity. The charge transport properties of the composites were examined by studying the electrical properties of the composites using the cyclic voltammetric measurements (CV) and temperature-dependent DC conductivity

within 300-500 K.

Experimental

The procedure for the synthesis of the PANI-GNP and PANI-GNP-GO composites was introduced in detail in our earlier report.[22] An aqueous solution of 0.5 M aniline hydrochloride monomer and 0.75 M $HAuCl_4$ were prepared. The monomer solution was slowly added to the $HAuClO_4$ solution. The mixture was stirred for ~30 min to initiate polymerization. A green solution was obtained. The mixture was stirred continuously for 5-6 h at room temperature to obtain a dark green precipitate. Using the same methods, the PANI-GNP-GO composite was synthesized by adding 25 wt % of GO to the monomer and stirring for 30 min before adding the oxidant to the monomer solution. The precipitated powder was filtered and washed with hot deionized water and acetone several times to remove the unreacted monomer and oxidant. The characterization techniques, preparation of thin films from the synthesized composites, and measurement of the DC electrical conductivity are similar to those described in previous studies.[23,24] Electrochemical experiments were carried out using a three-electrode system, in which platinum foils and saturated calomel electrodes (SCE) were used as counter and reference electrodes and 1.25 M H_2SO_4 as the electrolyte. Cyclic voltammetric measurements were performed at a scan rate of 10 mV/s, while temperature-dependent DC conductivity was measured in the pellet form of the composite between 300-500 K using the four-probe technique with a Keithly 224 constant current source and a Keithly 617 digital electrometer. The parallel surfaces of pressed pellets, 1.5 mm × 1.3 mm, were coated with gold through vacuum evaporation, and silver electrodes were placed on both surfaces using silver paste for better contact.

Results and Discussion

Characterization of the Composites Using XRD, XPS, and TGA. Figure 1 shows the XRD curves for GO, PANI-GNP, and PANI-GNP-GO composites. The diffraction peak of GO powder appeared around 26°, in relation to the *d*-spacing of graphene (0.425 nm) and graphene/graphene (0.39 nm). The broad peak centered at 2θ = 23° of the GO sample confirmed the random packing of graphene sheets in GO. A diffraction peak at 23-27° can be attributed to the (002) reflection of a hexagonal graphite structure and its intensity can reflect the degree of graphitization of a carbon material. Raw graphite shows a very strong (002) peak at 26°. For GO, despite a small change in the position of the principal reflection, the most striking difference is the intensity and broadness of the peak (observed at 2θ = 23°), corresponding to an average interlayer spacing of ~0.4 nm. The expansion of d-spacing relative to that of graphite is ascribed to the oxygen-containing groups and inserted H_2O molecules. Individual GOs are expected to be thicker than individual pristine graphene sheets due to the presence of

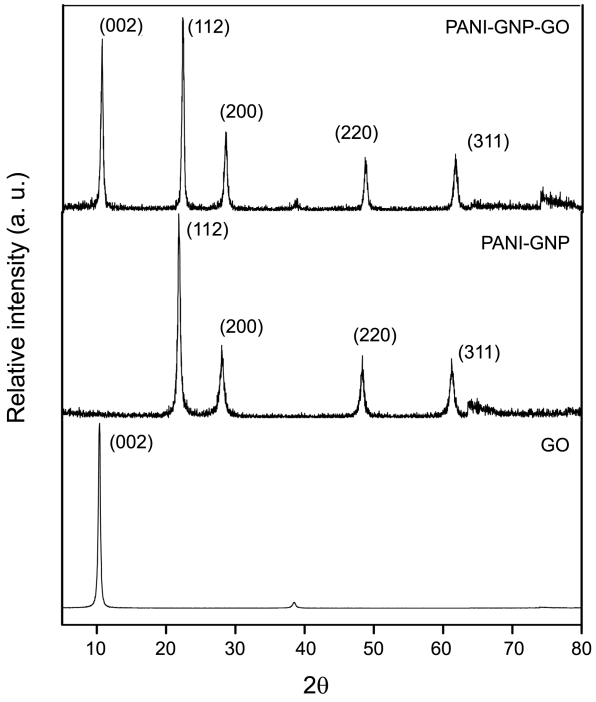

Figure 1. X-ray diffraction patterns for GO, PANI-GNP, and PANI-GNP-GO.

oxygen-containing functional groups attached to both sides of the graphene sheet and the atomic scale roughness arising from structural defects (sp3 bonding) generated on the originally atomically flat graphene sheets. In addition, the broad diffraction peak of the GO powder suggests that the functionalization process can influence the crystallinity of samples. This value is much larger than the *d*-spacing of natural graphite (0.34 nm). The appearance of the GO diffraction peak in PANI-GNP-GO confirms the presence and modification of the diffraction pattern of PANI-GNP-GO composite. The XRD pattern of PANI-GNP and PANI-GNP-GO are reflective of the presence of GNPs, PANI, and GO. The Bragg reflection patterns appearing at 2θ ~ 38° (111), 42° (20 0), 64° (220), and 78° (311) are indexed for the face-centered cubic, fcc structure of GNPs.[25,26] The peak centered at 2θ ~ 25° ascribed to the periodicity of the PANI chain[27] is absent in both PANI-GNP and PANI-GNP-GO; its disappearance may be due to the decrease in the amorphous nature of PANI in both PANI-GNP and PANI-GNP-GO composites.

Figure 2 shows the XPS spectra of GO, PANI-GNP, and PANI-GNP-GO. For GO, the C1s binding energy is approximately 285 eV and that of O1s is approximately 532 eV. The C1s spectra observed at 285 eV indicate a considerable degree of oxidation within the carbon atoms belonging to four functional groups, namely, the non-oxygenated ring C, C in the C-O bonds, the carbonyl C, and the carboxylate carbon (O-C=O).[28,29] The C1s spectra observed at 285 eV for GO is slightly decreased to 284.6 eV after the incorporation of GO to form PANI-GNP-GO. This result is probably due to the decrease in the conjugation as well as in the hydrogen bonds of the PANI backbone and the GO sheets. These

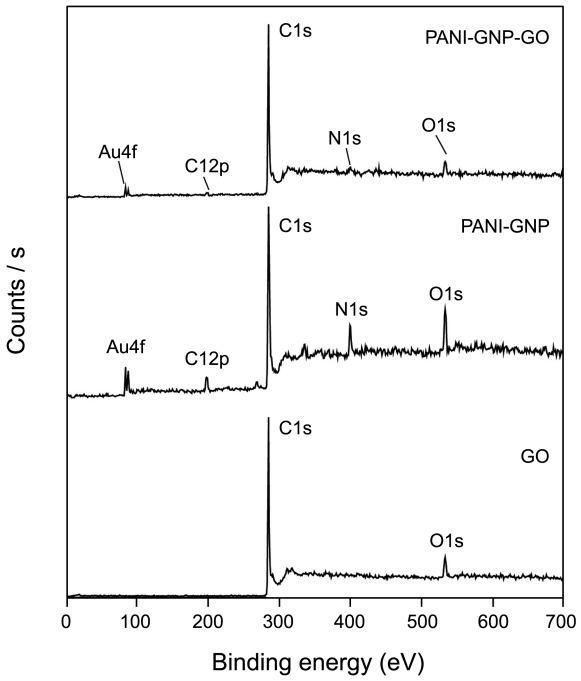

Figure 2. XPS spectra of GO, PANI-GNP, and PANI-GNP-GO.

interactions lead to a shift of the C-O-C and C-OH binding energies, and consequently resulted the modification of the two peaks into a new broad peak for the composite with the lower GO concentration. The other binding energies for PANI-GNP corresponding to Au4f, C12p, and N1s are observed at 81, 195, and 395.4 eV, respectively, whereas those for PANI-GNP-GO are at 81.7, 195.6, and 396.3 eV, respectively. The increases in the binding energies for Au4f, C12p, and N1s in PANI-GNP-GO may be due to the increase in the conjugation between PANI and GNPs because of the introduction of GO. These data show that a PANI-GNP-GO nanocomposite is formed.

Figure 3 shows the thermogravimetric curves for GO and the PANI-GNP and PANI-GNP-GO composites from room temperature to 800 °C. The TGA curve for GO does not show any decomposition patterns, whereas that for PANI-GNP exhibits three different stages of decomposition. The

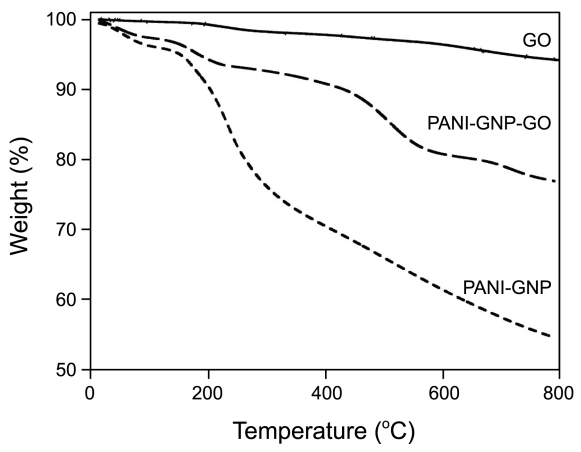

Figure 3. TGA curves for GO, PANI-GNP, and PANI-GNP-GO.

first stage is from room temperature to 200 °C and can be attributed to the water/moisture release. The second stage, from 200 to 350 °C, is due to the degradation of the skeletal PANI structure, and the third is due to the complete degradation of the polymer backbone. The PANI-GNP composite exhibits a residual weight of 55% (weight loss of 45%) at 800 °C, which may be due to the presence of GNPs in the PANI polymer. The degradation curve for PANI-GNP-GO is a hybrid of the PANI-GNP and GO curves. The degradation curves for PANI-GNP-GO are higher than those of PANI-GNP, with a residual weight of 77% (only 23% weight loss) at 800 °C, indicating the successful incorporation of GO in PANI-GNP.

Charge Transport Properties the Composites. Figure 4(a) shows the CV curves for GO, PANI-GNP, and PANI-GNP-GO composites obtained at 10 mV/s. The CV curve for PANI-GNP-GO is higher than those of pure GO and PANI-GNP. Compared with GO and PANI-GNP, PANI-GNP-GO exhibit greater current density response under same conditions. The enhanced electrochemical response of the PANI-GNP-GO nanocomposite is attributed to the surface modifications, as well as to the synergistic effect/charge-

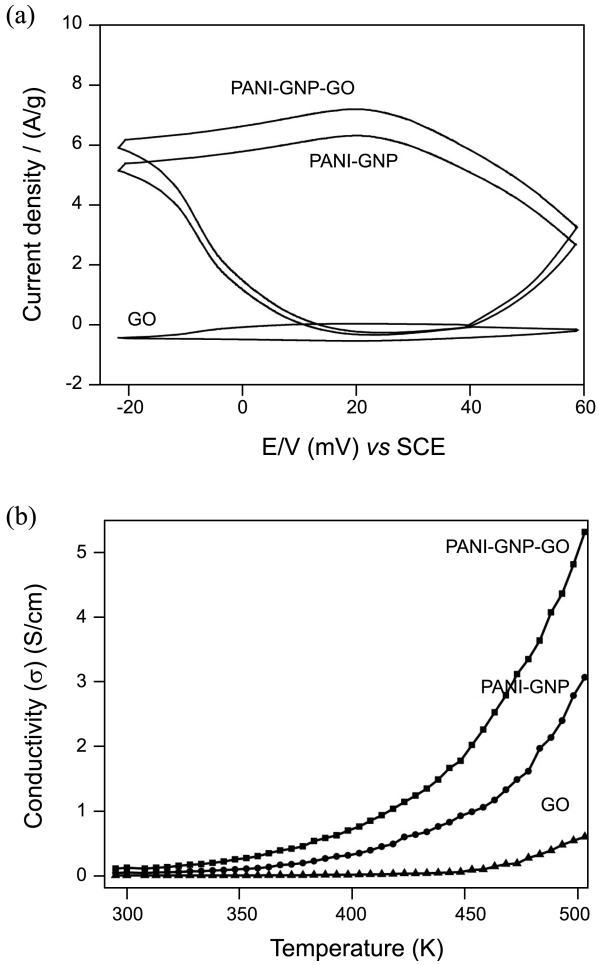

Figure 4. (a) CV curves for GO, PANI-GNP, and PANI-GNP-GO obtained at 10 mV/s, and (b) temperature-dependent DC conductivity of GO, PANI-GNP, and PANI-GNP-GO in the range of 300-500 K.

transport properties between GO and PANI-GNP, as observed from the spectral and surface modifications of the nano-composites as given in our earlier report.[19]

The temperature-dependent DC conductivity for the palletized GO, PANI-GNP, and PANI-GNP-GO were measured in the range of 300-500 K to facilitate further investigation of the charge-transport properties. The conductivity was increased with temperature almost linearly as shown in Figure 4(b). The conductivity values of GO, PANI-GNP, and PANI-GNP-GO beyond 300-500 K range from 7.08×10^{-5}–0.027, 0.004-0.31, and 0.01-0.53 S/cm, respectively. The conductivity values increase as the temperature increases, indicating a semiconducting behavior.[29,30] The conductivity values of the composites indicate that GO has a positive effect on conduction. This effect may be attributed to the modifications in the characterization of the composites, as demonstrated by the spectral characterization and surface imaging *via* XRD and XPS analysis.

Cyclic voltammetric and DC conductivity data indicate that the electrochemical response of PANI-GNP is increased by GO, which may be due to the increased interaction between PANI and GO in the PANI-GNP-GO composite.

Conclusions

The characterization of GO, PANI-GNP, and PANI-GNP-GO using XRD, X-ray photoelectron spectroscopy, and TGA analysis well supports the formation of the PANI-GNP and PANI-GNP-GO composites. The CV curve for PANI-GNP-GO was higher than those of pure GO and PANI-GNP, which indicating that GO has a positive role to the PANI-GNP composite regarding on the charge carrier transport properties. In addition, the temperature dependent DC conductivity obtained in the range 300-500 K range also showed higher value in the PANI-GNP-GO than those of PANI-GNP and pure GO, which means the increased interaction between PANI and GO in the PANI-GNP-GO composite. This result strongly suggests that the nano-composite has greater potential in the field of super-capacitors or other power source systems.

Acknowledgments. This research was supported by Environmental Engineering Development for the Next Generation grants sponsored by the Ministry of Environments in Korea (project No: 02-1-06-3-007).

References

1. Cao, Y.; Mallouk, T. E. *Chem. Mater.* **2008**, *20*, 5260.
2. Wu, Q.; Xu, Y.; Yao, Z.; Liu, A.; Shi, G. *ACS Nano* **2010**, *4*(4), 1963.
3. Basavaraja, C.; Kim, N. R.; Jo, E. A.; Huh, D. S. *J. Polym. Res.* **2010**, *17*, 861.
4. Liu, D. Y.; Reynolds, J. R. *ACS Appl. Mater. Interfaces* **2010**, *2*(12), 3586.
5. Jang, J.; Bae, J.; Choi, M.; Yoon, S. H. *Carbon* **2005**, *43*, 2730.
6. Cao, Y.; Mallouk, T. E. *Chem. Mater.* **2008**, *20*, 5260.
7. Tung, N. T.; Khai, T. V.; Jeon, M.; Lee, Y. J.; Chung, H.; Bang, J. H.; Sohn, D. *Macromol. Res.* **2011**, *19*(2), 203.
8. Swami, A.; Kumar, A.; Selvakannan, P.; Mandal, S.; Pasricha, R.; Sastry, M. *Chem. Mater.* **2003**, *15*, 17.
9. Jordan, R.; West, N.; Ulman, A.; Chou, Y. M.; Nuyken, O. *Macromolecules* **2001**, *34*, 1606.
10. Selvan, S. T.; Spatz, J. P.; Klok, H. A.; Möller, M. *Adv. Mater.* **1998**, *10*, 132.
11. Lee, J.; Sundar, V. C.; Heine, J. R.; Bawendi, M. G.; Jensen, K. F. *Adv. Mater.* **2000**, *12*, 1102.
12. Corbierre, M. K.; Cameron, N. S.; Sutton, M.; Mochrie, S. G. J.; Lurio, L. B.; Ruhm, A.; Lennox, R. B. *J. Am. Chem. Soc.* **2001**, *123*, 10411.
13. Mallick, K.; Witcomb, M. J.; Scurrell, M. S.; Strydom, A. M. *Gold Bulletin* **2008**, *41*(3), 246.
14. Zhang, K.; Zhang, L. L.; Zhao, X. S.; Wu, J. *Chem. Mater.* **2010**, *22*, 1392.
15. Kim, H.; Abdala, A. A.; Macosko, C. W. *Macromolecules* **2010**, *43*, 6515.
16. Wang, G.; Wang, B.; Park, J.; Yang, J.; Shen, X.; Yao, J. *Carbon* **2010**, *47*, 68.
17. Cote, L. J.; Silva, R. C.; Huang, J. *J. Am. Chem. Soc.* **2009**, *131*(31), 11027.
18. Basavaraja, C.; Kim, W. J.; Kim, Y. D.; Huh, D. S. *Mater. Lett.* **2011**, *65*, 3120.
19. Basavaraja, C.; Kim, W. J.; Kim, D. G.; Huh, D. S. *Mater. Phys. Chem.* **2011**, *129*, 787.
20. Basavaraja, C.; Veeranagouda, Y.; Lee, K.; Pierson, R.; Huh, D. S. *J. Polym. Sci. B: Polym. Phys.* **2009**, *47*, 36.
21. Waltman, R. J.; Pacansky, J.; Bates, C. W. J. *Chem. Mater.* **1993**, *5*(12), 1799.
22. Liu, Z.; Wang, Z. M.; Yang, X.; Ooi, K. *Langmuir* **2002**, *18*, 4926.
23. Park, S.; Dikin, D. A.; Nguyen, S. T.; Ruoff, R. S. *J. Phys. Chem. C* **2009**, *113*, 15801.
24. Pouget, J. P.; Jozefowicz, M. E.; Epstein, A. J.; Tang, X.; Macdiarmid, A. G. *Macromolecules* **1991**, *24*, 779.
25. Joint Committee on Powder Diffraction Standards, Diffraction data file: JCPDS International Center for Diffraction Data: Swarthmore, PA 1991.
26. Leff, D. V.; Brandt, L.; Heath, J. R. *Langmuir* **1996**, *12*, 4723.
27. Moon, Y. B.; Cao, Y.; Smith, P.; Heeger, A. J. *Polymer Commun.* **1989**, *30*, 196.
28. Becerril, H. A.; Mao, J.; Liu, Z.; Stoltenberg, R. M.; Bao, Z.; Chen, Y. *ACS Nano* **2008**, *2*, 463.
29. Yang, X.; Zhang, X.; Ma, Y.; Yi, H.; Wang, Y.; Chen, Y. J. *Mater. Chem.* **2009**, *19*, 2710.
30. Leff, D. V.; Brandt, L.; Heath, J. R. *Langmuir* **1996**, *12*, 4723.